Polymer 50 (2009) 3037–3046

Contents lists available at ScienceDirect

Polymer

journal homepage: www.elsevier.com/locate/polymer

Transesterification-controlled compatibility and microfibrillation in PC–ABS composites reinforced by phosphorus-containing thermotropic liquid crystalline polyester

Li Chen [a], Heng-Zhen Huang [a], Yu-Zhong Wang [a,*], Jinder Jow [b], Kenny Su [b,c]

[a] Center for Degradable and Flame-Retardant Polymeric Materials (ERCEPM-MoE), College of Chemistry, State Key Laboratory of Polymer Materials Engineering, Sichuan University, Chengdu 610064, China
[b] The DOW Chemical Company, 2301 N. Brazosport Blvd., Freeport, TX 77541, USA
[c] The DOW Chemical Taiwan Ltd., 17 Ren Jen Road, Hukou, Hsinchu 303, Taiwan, China

ARTICLE INFO

Article history:
Received 31 January 2009
Received in revised form
21 March 2009
Accepted 10 April 2009
Available online 24 April 2009

Keywords:
Transesterification
Compatibility
Thermotropic liquid crystalline polyester

ABSTRACT

For polymer/liquid crystal polymer (LCP) blend systems, the *in-situ* fibrillation of LCP in polymer matrix can result in the self-reinforcement of polymer/LCP composites. How to control the microfibrillation of LCP in matrix is a key to enhance the mechanical properties of composites. In this paper, we investigated the transesterification-controlled compatibility and microfibrillation of phosphorus-containing thermotropic liquid crystalline polyester, poly(*p*-hydroxybenzoate-*co*-DOPO-hydroquinone ethylene terephthalate) (PHBDET) in the PC/acrylonitrile–butadiene–styrene copolymer blend (PC–ABS) during the melt processing. A standard mode and temperature-modulated differential scanning calorimetry (DSC and TMDSC) and ^{13}C nuclear magnetic resonance (^{13}C NMR) were used to investigate the transesterification and compatibility of PHBDET with PC–ABS. Microstructures, rheological and mechanical properties of the composites were also studied via scanning electron microscopy (SEM), dynamic rheological measurement and universal material testing machine. The results showed that the extent of transesterification could influence the compatibility of PHBDET with PC–ABS, and could be controlled by processing temperature and time. The improved compatibility was not always favorable for the microfibrillation of PHBDET in PC–ABS, but a certain extent of transesterification showed a positive influence on the tensile properties of the composites. Therefore, there existed an optimal extent of transesterification, in which the composite could show a good balance of compatibility and tensile properties.

1. Introduction

Aromatic polycarbonates (PC), particularly for bisphenol A ones, are widely known engineering thermoplastics for many applications due to their outstanding mechanical properties, heat resistance, dimensional stability, transparency and exceptional clarity [1,2]. Further, in order to inhibit the notch-sensibility and improve melt processability and impact toughness which can be decreased radically with PC aging, elastomeric polymers such as styrene–butadiene–styrene triblock copolymer (SBS) or styrene–acrylonitrile binary copolymer (SAN) are typically added to PC. However, the most common blend is a blend with PC and acrylonitrile–butadiene–styrene copolymer (ABS), PC–ABS [2–4]. To provide a useful balance of toughness, heat resistance, and ease of processing at a lower cost, the optimal content of PC is in the range of 60–80 wt.%, and the mechanical properties vary with the composition of the blend [5,6].

Generally, plastics reinforcement can be achieved by mixing fibrous fillers, including natural fibers, carbon and glass fibers, mineral whiskers and carbon nanotubes into the plastic matrices [7–9]. Thermotropic liquid crystalline polyesters (TLCPs), particularly for the wholly aromatic ones, with high strength, stiffness and chemical resistance, good dimensional stability and low linear thermal expansion coefficient make them attractive as high performance engineering materials to offer numerous applications since their arrival [10,11]. Also, the presence of rigid structures in the oriented direction possessed inimitable performances including high modulus in its solid state and low melt viscosity in its molten state. Hence, as a dispersed phase in an engineering plastic, it can significantly alter the mechanical properties of the blended materials by the orientation of the rigid or semirigid chains of TLCP as a kind of organic *in-situ* reinforcing fillers during

* Corresponding author. Tel./fax: +86 28 85410259.
E-mail address: yzwang@email.scu.edu.cn (Y.-Z. Wang).

0032-3861/$ – see front matter © 2009 Elsevier Ltd. All rights reserved.
doi:10.1016/j.polymer.2009.04.026

processing. Various types of TLCPs, such as Vectra™ [12], have been reported to blend with polypropylene (PP), polycarbonate (PC), and poly(ethylene terephthalate) (PET), etc. to form the so-called *in-situ* reinforced composites [13,14].

However, molecular chains of main-chain TLCP exhibit a very stiff and rigid-rod nature [15]. A rigid-rod polymer showed a positive enthalpy value as it was blended with a flexible-chain polymer, and the small increase in entropy due to the blending in these two polymers was not able to compensate for the enthalpy effect. The free energy of blending is therefore positive. In other words, the compatibility between TLCPs and flexible-chain polymers is not favorable in thermodynamics. Phase separation of TLCP reinforced composites occurred where high-stress and high-temperature conditions encountered, which has long been a real threat to limit their wider applications [16–18]. Generally, processing or thermal treating of polyesters, particularly at high temperature near or above their melting points, can have acidolysis by acid-end groups, alcoholysis by hydroxyl-end groups, or mid-chain ester–ester interchange reaction with themselves or others [19,20]. Since the aforementioned reactions (so-called transesterification), had been detected in polycondensation chemistry, a number of investigations focused on transesterification between two incompatible components have been carried out to prevent phase separation and hereby to enhance mechanical properties of the multi-phase composites. There are two different viewpoints on the sequence of events that produced a compatible composite while two incompatible components are mixed; one considers that the transesterification between two thermoplastic polyesters is a necessary step to obtain a compatible one [21]; and another claims that the intermolecular mixing between two polyesters might first occur followed by transesterification, which means transesterification might not be an essential step to obtain a compatible composite [22,23].

Many researchers investigated transesterification between TLCP and polycarbonate, and reported the relationships between transesterification and mechanical properties as well as morphology of the reinforced composites [18,21,24–30]. However, it was difficult to control this chemical reaction during processing [30]. On the other hand, TLCP fibrils were thermodynamically unstable and hence trended to relax or to break up at temperatures above the melting point of TLCP [31], which made the *in-situ* fibrillation of the TLCP droplets becoming unattainable. Therefore, one question should be raised as to whether measurable transesterification could essentially occur during melt processing of a TLCP/PC binary or a TLCP/PC–ABS ternary composite. And if so, the following question is how to control such transesterification within an acceptable extent to enhance the fibrillation of TLCP droplets in the composite. For such purposes, a unique phosphorus-containing TLCP with methylene flexible spacers to reduce its thermal transition temperature and to increase the solubility and mixing entropy [32,33], has been employed into PC–ABS to investigate the above questions. Because in PC–ABS, ABS could be considered as an inert component which could not react with two kinds of polycondensates during melt processing, transesterification would occur only between PC and TLCP. In this article, this unique TLCP was poly(*p*-hydroxybenzoate-*co*-DOPO-hydroquinone ethylene terephthalate), defined as PHBDET [34], synthesized from *p*-acetoxybenzoic acid, terephthalic acid, ethylene glycol and 2-(6-oxido-6*H*-dibenz⟨c,e⟩⟨1,2⟩-oxaphosphorin-6-yl)-hydroquinone. ^{13}C NMR was introduced to determine the extent of transesterification of each composite prepared at different processing conditions. Also, standard mode and temperature modulated DSC (TMDSC) were introduced to determine the changes of compatibility between two polycondensates, which were greatly affected by the extent of transesterification. Hereby, fibrillation morphologies of the composites with different compatibilities were discussed through scanning electronic microscopy (SEM). Furthermore, rheological performances and tensile properties of the samples affected by the extent of transesterification were also presented and discussed.

2. Transesterification statistic analysis

Since the high-resolution solution NMR spectroscopy has been introduced as an efficient method to detect the chain structure and the sequence distribution of the polymers, it has received wide application to determine quantitatively the extent of transesterification of the two different polyesters before and after blending [35]. Similar to the analyses in PES/PET by Yamadera [36] and in PC/PBT by Devaux [37], two different polycondensates, PHBDET and PC in this case, were divided into four components, and each component with different chemical structure but the same functionality was represented as A_i ($i = 1, 2$) and B_j ($j = 1, 2$).

Over two decades ago, Devaux and his co-workers [36] developed a statistic analysis of the structure of four-component co-polycondensates resulting from transesterification between two polycondensates with different chemical characteristics via ^{13}C NMR. In their investigation, six parameters were applied to describe the four-component co-polycondensate formed via transesterification between two linear polycondensates, $(A_1B_1)_p$ and $(A_2B_2)_q$, as summarized below:

$$\left[(A_1 - B_1)_x - (A_2 - B_1)_y\right]_m - \left[(A_1 - B_2)_z - (A_2 - B_2)_w\right]_n$$

where A_1 and A_2, and B_1 and B_2, symbolize the monomer units with different chemical structures but with the same functionality, and p and q refer to the number-average degrees of polymerization of two linear polycondensates, respectively; in the four-component one, x, y, z, and w represent the average lengths of the various molecular sequences; and m and n represent the mean lengths of co-components having the same B_1 or B_2 unit in common. Molar fractions of both A_i ($i = 1, 2$) and B_j ($j = 1, 2$) units are defined by the concentration ratios as below:

$$F_{A_i} = [A_i] / \sum_{i=1}^{2} [A_i]$$

$$F_{B_j} = [B_j] / \sum_{j=1}^{2} [B_j]$$

For two-component dyad analysis, the molar fraction of the dyads A_iB_j ($i, j = 1, 2$) would be:

$$F_{A_iB_j} = [A_iB_j] / \sum_{i,j=1}^{2} [A_iB_j] = [A_iB_j] / \sum_{i=1}^{2} [A_i]$$

And the probability of finding an A_i unit followed by a B_j unit is defined as follows:

$$P_{A_iB_j} = [A_iB_j] / \sum_{j=1}^{2} [A_iB_j] = [A_iB_j] / [A_i] \; (i, j = 1, 2)$$

Similarly, the probability of finding a B_j unit followed by an A_i unit is given by:

$$P_{B_jA_i} = [B_jA_i] / \sum_{i=1}^{2} [B_jA_i] = [B_jA_i] / [B_j] = [A_iB_j] / [A_j] \; (i, j = 1, 2)$$

Therefore, based on the above equations, the degree of randomness β is defined as follows:

$$\beta = P_{A_iB_j} + P_{B_jA_i} \ (i,j = 1,2; i \neq j)$$

Therefore, below is the list of five presumptions to define the structural sequences of the blending composites as Han and his co-workers concluded [21]:

$\beta = 0$ suggests a co-polycondensate with long sequences or a simple physical mixture of two individual polycondensates.
$\beta < 1$ denotes that the repeating units tend to accumulate into homogeneous sequences such as A_1B_1 and A_2B_2, rather than randomly distribute.
$\beta = 1$ demonstrates that the repeating units are randomly dispersed in the co-polycondensate obeying the Bernoulli statistics.
$\beta > 1$ indicates a tendency of A_1B_2 and A_2B_1 sequences instead of the homogeneous sequences as A_1B_1 and A_2B_2.
$\beta = 2$ represents very long alternate sequences such as A_1B_2 and A_2B_1 formed during transesterification.

3. Experimental part

3.1. Materials and preparation of PC–ABS/PHBDET composites

The PC–ABS (4:1 in weight ratio) used here was kindly provided by Dow Chemical Company and dried under vacuum at 100 °C for 24 h before processing. A phosphorus-containing TLCP based on *p*-hydroxybenzoic acid, 2-(6-oxido-6*H*-dibenz⟨c,e⟩⟨1,2⟩-oxaphosphorin-6-yl)-hydroquinone, terephthalic acid, and ethylene glycol, defined as PHBDET used in this study, was synthesized following the procedures described in our previous work [34,38]. $(100 - X)/X$ PC–ABS/PHBDET composites, in which X referred to the weight percentage of PHBDET in the range from 10 to 25 wt.%, were prepared by melt processing using a HAAKE Rheomex 254 twin-screw extruder together with a HAAKE Postrx to squeeze out flake specimens with 1 mm thickness, at different temperatures above the flow temperature of PHBDET with varied durations of time from 4 to 10 min.

3.2. Thermal transition analyses

Thermal transition temperatures of all composites were measured using a differential scanning calorimeter (DSC TAQ200 1747) with 5 ± 0.25 mg of samples under a nitrogen atmosphere at a flow rate of 50 mL/min. The instrument was calibrated for both heat flow and temperature using indium and zinc standards. For standard mode, testing schedules were as follows: first these specimens were heated from 40 to 260 °C at a heating rate of 20 °C/min and isothermal for 5 min, and then quenched to 40 °C; then they were heated again to 300 °C at the same heating rate. For temperature modulated (TM) conventional mode, specimens underlying a heating rate of 2.5 °C/min was typically used with the modulation amplitude of the sinusoidally varying temperature of 0.5 °C of every 60 s to obtain the TMDSC thermograms. Midpoint of the glass transition was determined to the glass transition temperature (T_g) of the sample. All thermograms were recorded from the second heating cycle to minimize adverse influence from thermal history of the sample during preparation.

3.3. ^{13}C NMR analyses

In this article, solution-state ^{13}C NMR was used to determine chemical reactions between each component of the 85/15 PC–ABS/PHBDET composites during processing. Specimens of 25 mg were dissolved in 1.0 mL of $CF_3COOD/CDCl_3$ (9:1 in volume) solvent. All chemical shifts were reported in ppm downfield from tetramethylsilane (TMS) which was used as an internal standard. ^{13}C NMR spectra of the composites were performed on a Bruker Avance 400 MHz operated at a resonance frequency of 100.5 MHz. Structures of two dyads A_1B_1 and A_2B_2 are summarized in Fig. 1 with various carbons coded.

3.4. Morphology and tensile properties

In order to observe the morphologies of the composites, the fractured surface of 85/15 PC–ABS/PHBDET composites prepared during melt processing at 260 °C for various durations were observed by an FEI (INSPECT F) SEM instrument with an acceleration voltage of 10 kV. The observed specimens were prepared by cryogenically fracturing in liquid nitrogen. Gold was sprayed on the fractured phase surface before observation.

Tensile properties of the samples were measured via a universal material testing machine (CMT6503, Shenzhen SANS Test Machine Co., Ltd.) according to ISO 527-5: 1997 (Plastics-Determination of tensile properties – Part 5: Test conditions for unidirectional fibre-reinforced plastic composites). The values of tensile properties reported here were the averages of at least five separate measurements.

3.5. Rheological analyses

An Advanced Rheometric Expansion System (Bohlin Gemini 200) was used in the oscillatory shear mode with a parallel-plate fixture (8 mm diameter and 1 mm thickness) to conduct dynamic frequency sweep experiments. The complex viscosity ($|\eta^*|$), dynamic storage modulus (G') and dynamic loss modulus (G'') were measured as functions of angular frequency (ω) ranging from 0.02π to 200π rad/s at 250 ± 0.2 °C. Strain amplitude varied from 0.01 to 0.06, which was found to be well within the linear viscoelasticity range of the materials investigated.

4. Results and discussion

4.1. Transesterification in PC–ABS/PHBDET composites

4.1.1. Thermal transitions in PC–ABS/PHBDET composites

Standard mode DSC thermograms for both PC–ABS and PHBDET are shown in Fig. 2. It could be observed that PC–ABS was a glassy

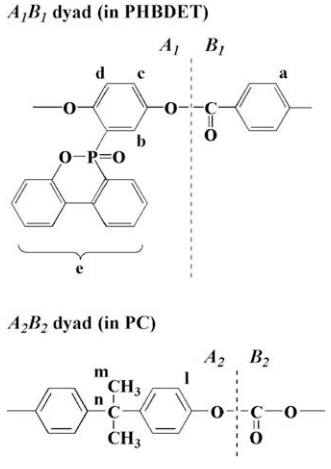

Fig. 1. A_1B_1 and A_2B_2 dyads in PHBDET and PC, respectively.

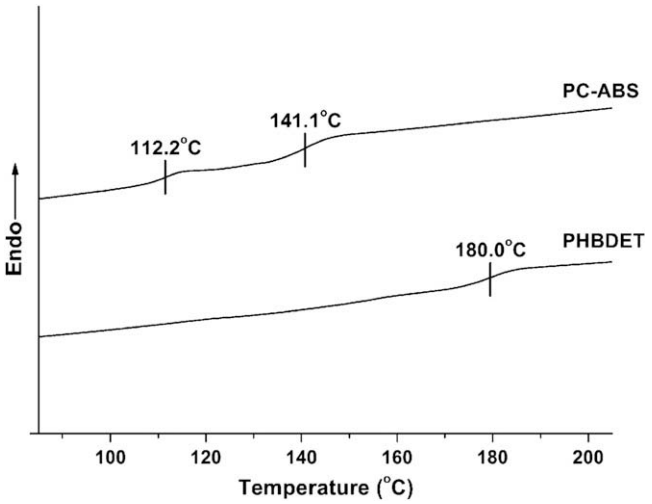

Fig. 2. DSC thermograms at a heating rate of 20 °C/min in the second heating cycle for PC–ABS and PHBDET.

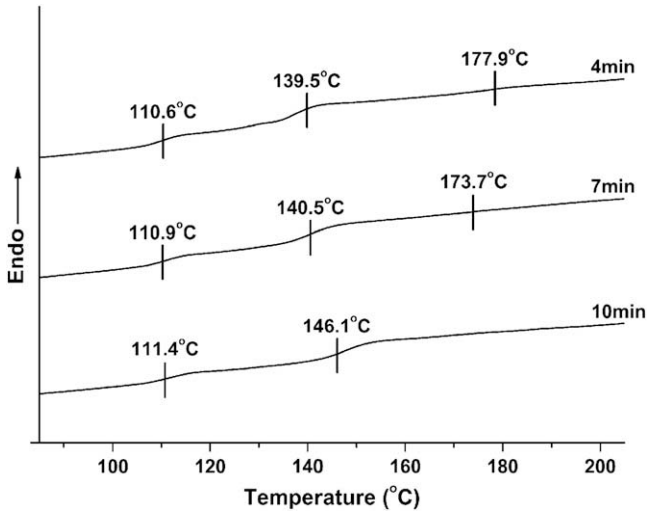

Fig. 4. DSC thermograms at a heating rate of 20 °C/min in the second heating cycle for 85/15 PC–ABS/PHBDET by melt blending at 260 °C for various durations.

polymer blend with two glass transitions at 112.2 and 141.1 °C, the lower T_g belonged to SAN phase of ABS, while the higher one should be assigned to PC. In addition, PHBDET is a kind of random liquid crystalline copolyester with a single T_g at 180.0 °C.

DSC thermograms for 85/15 PC–ABS/PHBDET composites prepared by melt processing for 7 min at various temperatures ranging from 240 to 270 °C are shown in Fig. 3. After blended with PHBDET at 240 °C for 7 min, the blends had the third endothermal transition, which should be recognized as the glass transition of PHBDET, at 179.8 °C, much similar to that of the original PHBDET; the two lower T_gs separated by 27.9 °C, which was slightly decreased from 28.9 °C of PC–ABS. Also, the endothermal inflexion related to PC phase was shifted from 141.1 °C to the lower temperature at 138.6 °C. As the blends were prepared at higher temperature for the same duration, the two higher T_gs which attributed to PC and PHBDET trended to converge on each other, and finally converged into one single higher T_g appearing at 145.1 °C as the processing temperature raised up to 270 °C.

Fig. 4 shows DSC thermograms for 85/15 PC–ABS/PHBDET composites prepared by melt processing at 260 °C for various durations altering from 4 to 10 min. Similar to the temperature effect summarized in Fig. 3, the two higher T_gs related to PC and PHBDET were closer to each other as processing time increased, and formed one single T_g appeared at 146.1 °C as the processing duration reached to 10 min. Confluence of two separate glass transition implied an improvement of the compatibility in the PC–ABS/PHBDET composites processed at higher temperature or for longer duration.

In this case, the single T_g of a totally compatible binary composite could be predicted by the Fox equation [39,40] as follows:

$$1/T_g = w_1/T_{g,1} + w_2/T_{g,2}$$

where T_g is the observed glass transition temperature of the copolymer or the blend, w_1 is the weight fraction of component 1 having a glass transition temperature at $T_{g,1}$, while w_2 indicates the weight fraction of component 2 having a glass transition temperature at $T_{g,2}$. In PC–ABS, ABS could be considered as an inert component which could not react with two kinds of polycondensates during melt processing. Hereby, a transesterification-induced compatibility should only occur between PC and PHBDET.

Additionally, based on the consideration of transesterification which would take place during melt processing, the molecular chain composition of both two polycondensates could be changed to a certain extent to form somehow a kind of random copolymer. Hereby the Gordon–Taylor equation [41,42] was applied to predict the single T_g of a random copolymer based on two copolymerized monomers as follows:

$$T_g = \frac{T_{g,1} + (KT_{g,2} - T_{g,1})w_2}{1 + (K-1)w_2}$$

where T_g is the observed glass transition temperature of PC–ABS/PHBDET and K is a fitting parameter for the random copolymer.

In Fig. 5, T_g values of the composite with various PHBDET contents after 10 min of blending at 260 °C were plotted, along with the predictions of the Fox and the Gordon–Taylor equations with a fitting parameter of $K = 0.70$. In such case, before the calculation, the content of ABS has been already excluded as an inert component, and the weight fraction of PHBDET has been renormalized. Values calculated from the Fox equation were slightly higher than those of the experimental ones, which was

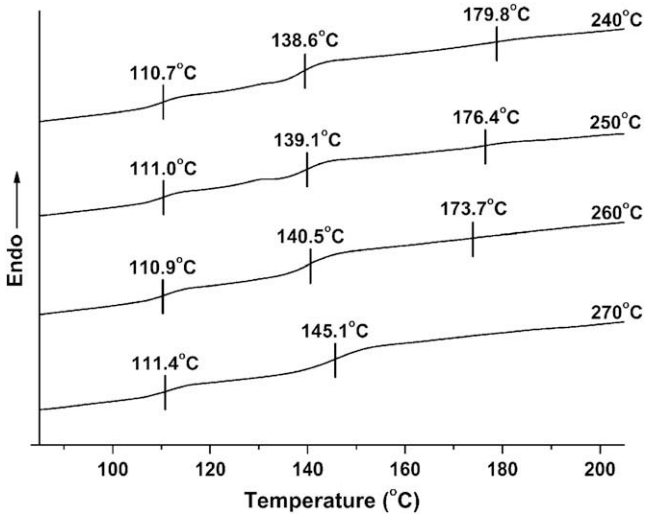

Fig. 3. DSC thermograms at a heating rate of 20 °C/min in the second heating cycle for 85/15 PC–ABS/PHBDET by melt blending at various temperatures for 7 min.

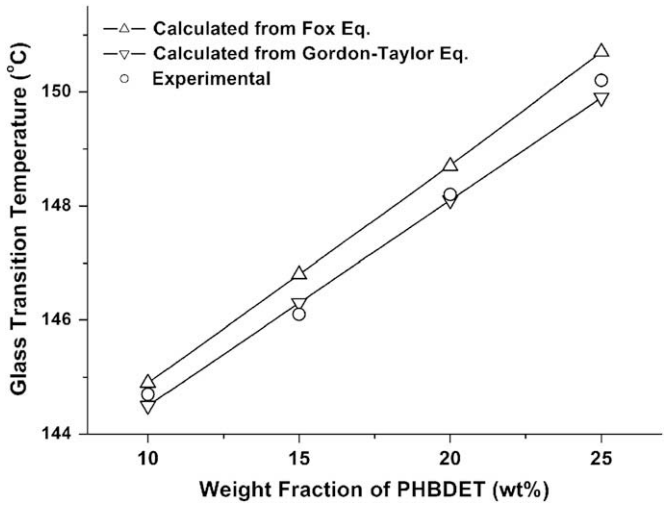

Fig. 5. Calculated and experimental glass transition temperatures of PC–ABS/PHBDET containing various content of PHBDET melt processed at 260 °C for 10 min.

quite opposite to the results reported by Wei et al. before [27]. Generally, two possible factors might be used to explain these differences. One was that when the transesterification occurred, a certain amount of macromolecular rearrangement would take place to increase the randomness of the polycondensates and hence to influence the glass transition temperature. Another was that byproducts with relatively lower molecular weight formed during transesterification played as plasticizers to reduce the glass transition temperature of the composites. However, it was clear that the results from the Gordon–Taylor equation fitted better to the experimental data than those from the Fox equation. This indicates that the transesterification-controlled compatible composites were much similar to a random copolymer with fine compatibility between each component rather than a totally physically compatible composite. Also, due to the presence of the bulky pendent side group in PHBDET as a steric effect, it would take more time for the transesterification to be completed at higher composition of PHBDET.

Table 1
Glass transition parameters for 85/15 PC–ABS/PHBDET prepared at 260 °C for different processing durations.

Processing duration (min)	T_g (°C)		$T_{g,i}$ (°C)[a]		ΔT (°C)[b]		ΔC_p (J/g °C)[c]
	PC	PHBDET	PC	PHBDET	PC	PHBDET	
4	135.8	163.9	124.6	156.9	28.5	16.6	0.192
7	142.9	162.2	131.5	160.1	32.4	14.5	0.236
10	145.1		134.1		48.2		0.407

[a] $T_{g,i}$ represents the onset temperature of the glass transition peaks.
[b] ΔT is defined as shown in Fig. 6.
[c] Values of ΔC_p at the temperature region of 120–170 °C are calculated as following: for the single transition system, ΔC_p calculated from the equation as $\Delta C_p = \int_{C_p(i)}^{C_p(e)} [dC_p(T)/dT]dT$; for the multi-peaks system, $\Delta C_p = w_1\Delta C_{p,1} + w_2\Delta C_{p,2}$ [43,44].

For further investigation on the compatibility between PC and PHBDET, TMDSC was introduced into such case. Fig. 6 presents the derivative of heat capacity (dC_p/dT) signals for PC–ABS/PHBDET obtained at different processing conditions as a function of the processing duration. Signal traces of PC–ABS/PHBDET prepared at 260 °C for 4 min with three individual transition peaks showed a physical mixture without evident compatibility, which presented a quite agreement with standard mode DSC result. As the processing duration was prolonged to 10 min, the two higher peaks which attributed to PC and PHBDET trended to converge on each other at 145.1 °C, suggesting a complete compatibility between PC and PHBDET phases. However, the composite prepared at 260 °C for 7 min showed a partial compatibility as the residual peak appeared at 162.2 °C which should be attributed to PHBDET. Table 1 summarizes values of T_g, ΔT and ΔC_p for 85/15 PC–ABS/PHBDET prepared at 260 °C for different processing durations. The increment of ΔC_p directly suggested the improvement of compatibility between PC and PHBDET as the processing duration increased.

4.1.2. ^{13}C spectroscopy of PC–ABS/PHBDET composites

Hereby, to obtain direct evidence for transesterification between PC and PHBDET, solution-state ^{13}C NMR spectroscopy for melt processed 85/15 PC–ABS/PHBDET composites was used. Two dyads A_1B_2 and A_2B_1 formed during melt processing with various carbons being coded are shown in Fig. 7.

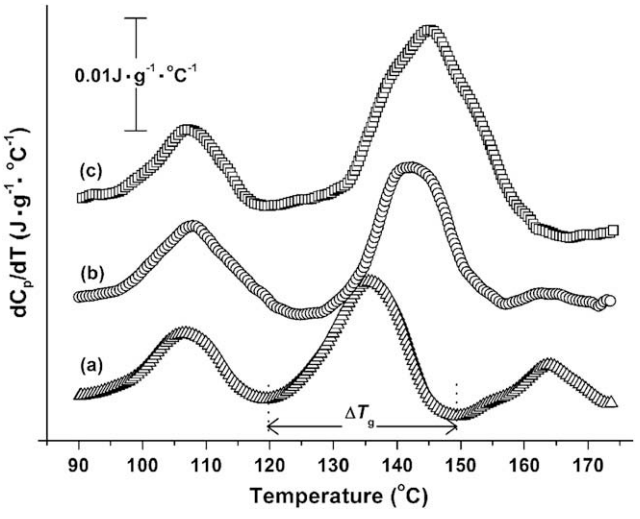

Fig. 6. dC_p/dT signals for 85/15 PC–ABS/PHBDET prepared at 260 °C for different processing durations: (a) for 4 min; (b) for 7 min; (c) for 10 min.

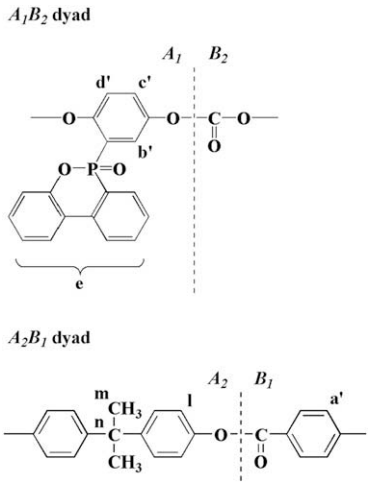

Fig. 7. A_1B_2 and A_2B_1 dyads formed during melt processing.

From the ^{13}C NMR spectra of PC–ABS, it could be noticed that a very large peak appeared at 31.04 ppm assigned to methyl carbon [C(m)] in A_2B_2 in PC phase, which was quite distinct from the aliphatic peaks at the region of 35–38 ppm corresponding to ABS phase. Also, from the ^{13}C NMR spectra of PHBDET, one might observe that a moderate peak at 121.65 ppm appeared near a strong and broad peak at the region of 120.0–121.5 ppm, in which the lower one should be assigned to C(d) and the higher one should be attributed to aromatic carbon C(a) of in A_1B_1 dyad of PHBDET, respectively.

During the melt processing, peaks at the region of 35–38 ppm corresponding to ABS almost remained the same, indicating ABS played as an inert component which did not react with two polycondensates during the melt processing. Also, with the fixed processing duration of 7 min and the processing temperature increased from 240 to 270 °C, peak at 31.04 ppm assigned to methyl carbon in PC phase was kept more or less constant as shown in Fig. 8. However, in Fig. 9, the peak at 121.65 ppm seemed to decrease, and simultaneously a new peak appeared at 123.22 ppm, and the relative intensity of the new peak gradually increased, which confirmed the occurrence and progress of transesterification between PC and PHBDET. Moreover, with a fixed processing temperature of 260 °C and the processing duration increased from 4 to 10 min, the peak at 121.66 ppm tended to decrease, and the new peak appeared at 123.22–123.24 ppm at the same time, which had the same assignments as those given aforementioned.

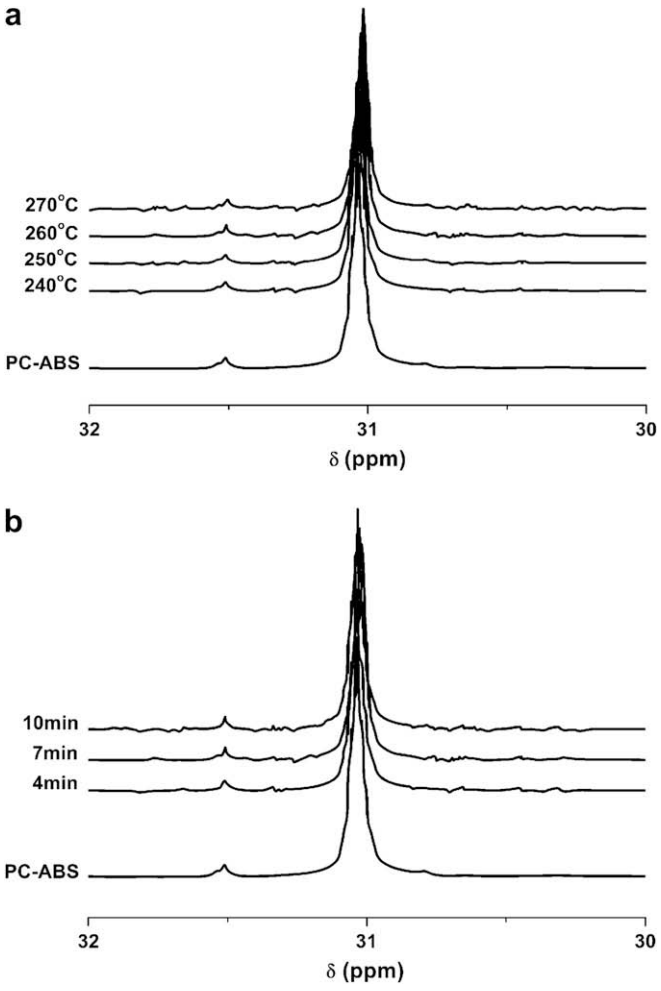

Fig. 8. ^{13}C NMR spectra (at 30–32 ppm region) of PC–ABS and PC–ABS/PHBDET: (a) obtained at different melt processing temperatures for 7 min; (b) at 260 °C for various durations.

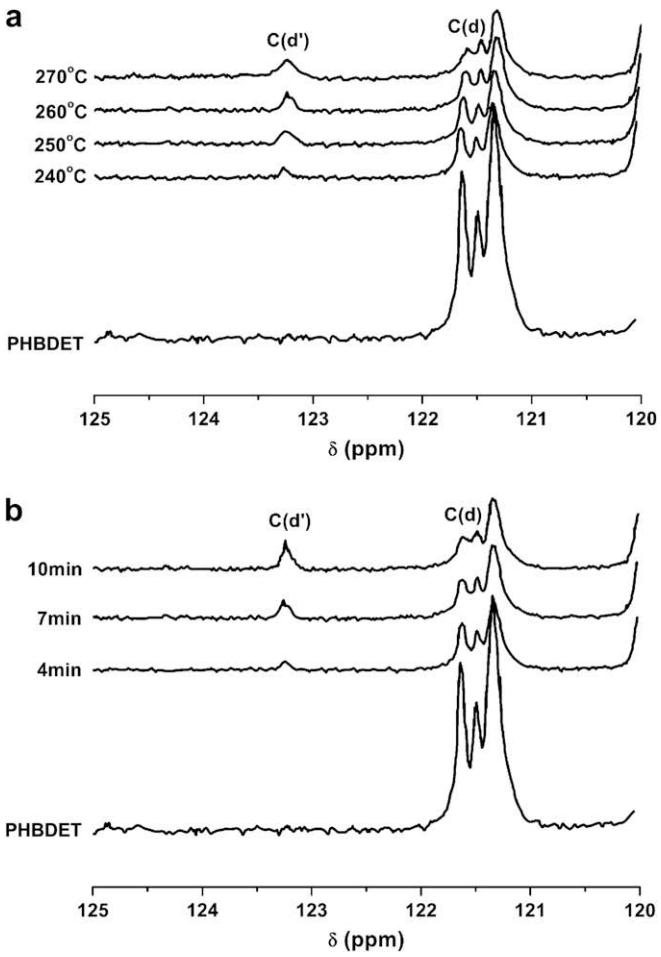

Fig. 9. ^{13}C NMR spectra (at 120–125 ppm region) of PHBDET and PC–ABS/PHBDET: (a) obtained at different melt processing temperatures for 7 min; (b) at 260 °C for various durations.

For simplifying the evaluation of the degree of randomness (β) from the ^{13}C NMR spectra, the relative intensities of only three kinds of carbons, including *meta*-position carbon from DOPO group in A_1B_1 dyad [C(d)] and in A_1B_2 dyad [C(d')], and methyl carbon in PC [C(m)], were investigated and listed in Tables 2 and 3. Based on the equations listed before, the degree of randomness (β) for the composites was evaluated and summarized in Tables 4 and 5. Fig. 10 shows the degree of randomness (β) evaluated from the ^{13}C NMR spectra as a function of processing conditions. Both curves suggested that an optimal degree of randomness occurred

Table 2
Relative intensities of ^{13}C NMR peaks for 85/15 PC–ABS/PHBDET composites prepared at various temperatures for 7 min.

Processing temperature (°C)	Relative intensity		
	d (121.65 ppm)	d' (123.22 ppm)	m (31.04 ppm)
240	0.41	0.04	5.25
250	0.37	0.11	5.27
260	0.29	0.16	5.22
270	0.26	0.22	5.19

Table 3
Relative intensities of ^{13}C NMR peaks for 85/15 PC–ABS/PHBDET composites prepared at 260 °C for various durations.

Processing duration (min)	Relative intensity		
	d (121.66 ppm)	*d′* (123.24 ppm)	*m* (31.06 ppm)
4	0.40	0.10	5.30
7	0.29	0.16	5.22
10	0.24	0.25	5.23

Table 4
Probability of $P_{A_iB_j}$ and degree of randomness (β) for 85/15 PC–ABS/PHBDET composites prepared at various temperatures for 7 min.

Processing temperature (°C)	$P_{A_1B_1}$	$P_{A_1B_2}$	$P_{A_2B_1}$	$P_{A_2B_2}$	β
240	0.95	0.05	0.01	0.99	0.06
250	0.86	0.14	0.03	0.97	0.17
260	0.67	0.33	0.03	0.97	0.36
270	0.60	0.40	0.04	0.96	0.44

as the processing temperature was high enough, or the melt processing time was long enough. However, the degree of randomness (β) was still less than 0.5 even when the composite was processed at 260 °C for 10 min, indicating that during the melt processing, it would form the mixtures with highly complicated structures rather than a statistical copolymer obeying the Bernoulli statistics. From the results tested at a lower processing temperature, one might conclude that the transesterification hardly occurred between PC and PHBDET in the composites when the specimens were melt processed at 240 °C, or at a higher temperature but for a relatively short duration. All results showed quite agreement with the phenomenon observed through DSC and TMDSC, indicating that a transesterification-controlled compatibility could take place under the appropriate processing condition.

4.2. Morphology, rheological and tensile properties of PC–ABS/PHBDET composites

4.2.1. Morphology of PC–ABS/PHBDET composites

It is well-known that TLCPs are easy to orient under shearing, and have a great trend to form elongated structures such as fibrils and ribbons via dynamic/thermodynamic driving force in thermoplastic matrices [13,45,46]. However, TLCP fibril was thermodynamically unstable and hence trended to relax or to break up during processing [31]. Furthermore, transesterification occurred during the melt processing complicated the morphology of the composites containing two or more kinds of polycondensates. Fig. 11 shows SEM fractographs of the squeezed-out flakes of PC–ABS/PHBDET composite with the direction parallel to the orientation. Fig. 11(a) and (b) exhibit the fractographs of the composite obtained by melt processing at 260 °C for 4 min. At a magnification of 12 000×, it was clear that PHBDET domains in Fig. 11(b) had an extremely high aspect ratio (about 15–20) and highly oriented

Table 5
Probability of $P_{A_iB_j}$ and degree of randomness (β) for 85/15 PC–ABS/PHBDET composites prepared at 260 °C for various durations.

Processing duration (min)	$P_{A_1B_1}$	$P_{A_1B_2}$	$P_{A_2B_1}$	$P_{A_2B_2}$	β
4	0.93	0.07	0.01	0.99	0.08
7	0.67	0.33	0.03	0.97	0.36
10	0.56	0.44	0.05	0.95	0.49

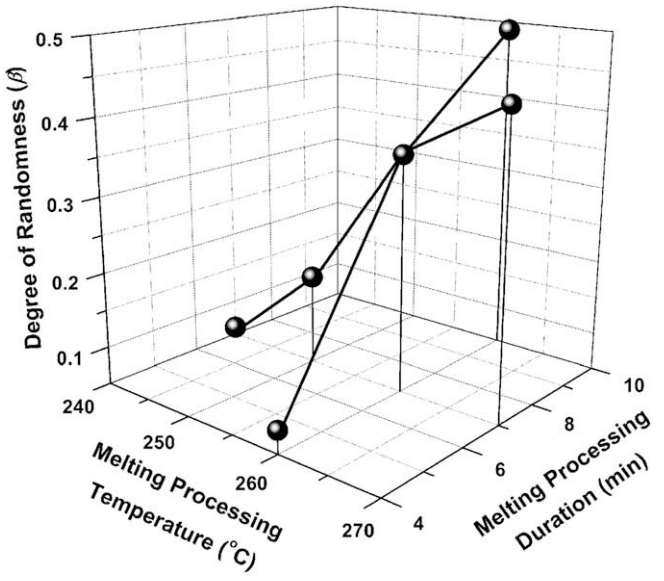

Fig. 10. Degree of randomness (β) evaluated from ^{13}C NMR spectra of 85/15 PC–ABS/PHBDET composite as a function of melt processing conditions.

along the squeezing direction. Also, due to the negligible extent of transesterification during the melt processing at 260 °C for 4 min, a very sharp interface between PC and PHBDET phases could be observed, indicating there was no such obvious diversification in the morphology of the composite occurring while the composite was melt processed for a relatively short duration, say for 4 min. However, the interface area became gradually diffused as the processing duration increased. Moreover, PHBDET microfibrils tapered, shortened and broke progressively as the processing duration was prolonged sequentially as shown in Fig. 11(e) and (f) and Table 6, indicating that the transesterification and the transesterification-controlled compatibility greatly affected the phase morphology of the composite.

4.2.2. Rheological studies of PC–ABS/PHBDET blends

To further investigate the rheological properties of PC–ABS/PHBDET composites related to transesterification during the melt processing, an ARES measurement was used in the oscillatory shear mode with a parallel-plate fixture to examine the rheological changes under shearing. Fig. 12(a) shows the complex viscosity plots of PC–ABS/PHBDET prepared at 260 °C for different duration times. It is noticeable that the processing duration as well as temperature considerably affected the complex viscosities of the composites while the processing temperature reached to a critical value. Fig. 12(b) indicates that the processing duration did not influence the complex viscosities as the melting temperature turned down to 240 °C. Combining the rheological and morphology observations, it was clear that transesterification significantly affect the macrocosmic distribution of PHBDET dispersed in PC–ABS matrix.

4.2.3. Tensile properties

Table 7 lists the tensile properties of squeezed-out flakes of 85/15 PC–ABS/PHBDET composites obtained at 260 °C for various processing duration times ranging from 4 to 10 min. For comparison, tensile properties of PC–ABS were examined after processing with the same apparatus at 260 °C for 7 min. Tensile strength of the composites slightly increased with the increase in the processing duration, and then sharply decreased from almost 53 MPa to

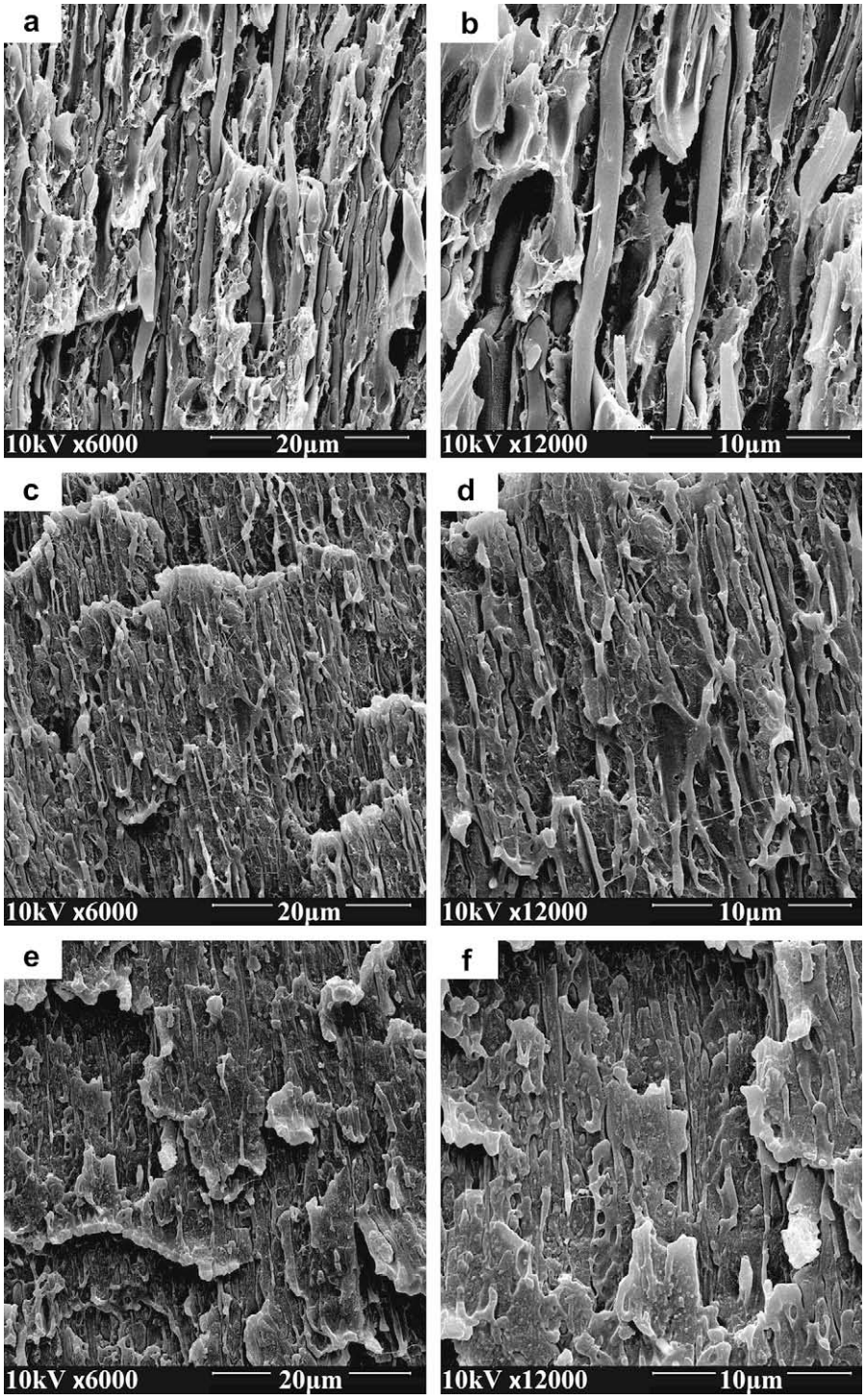

Fig. 11. Scanning electron micrographs of the cryogenically fractured surfaces of squeezed-out flakes prepared at 260 °C with a direction longitudinal to the orientation: [(a), (b)] for 4 min, [(c), (d)] for 7 min, and [(e), (f)] for 10 min.

42 MPa as the duration reached to 10 min. Han and his co-workers [21] suggested that there did exist a critical value for the degree of randomness β, and it kept increasing with the melt processing duration extended as NMR results indicated, thus the ability for TLCP to function as a reinforcing agent for PC continued to decrease when β exceeded a certain critical level, which was corresponding to changes of the microfibrillation morphologies of the composite. However, the elongation at break became much smaller in all composites, which failed in a more brittle behavior beyond the yield point. Apparently the microfibrillation of PHBDET in the composites greatly affected the elongation at break of the PC–ABS/PHBDET composites due to the lower ductility in the composites, which was resulted from the higher reduction of the molecular mobility of the matrix [47]. In this case, a partially compatible

Table 6
The average size of PHBDET microfibrils in 85/15 PC–ABS/PHBDET composites obtained during melt processing at 260 °C for different durations.

Size (μm)	4 min	7 min	10 min
Length	18.87	11.69	7.54
Diameter	1.22	0.56	0.32

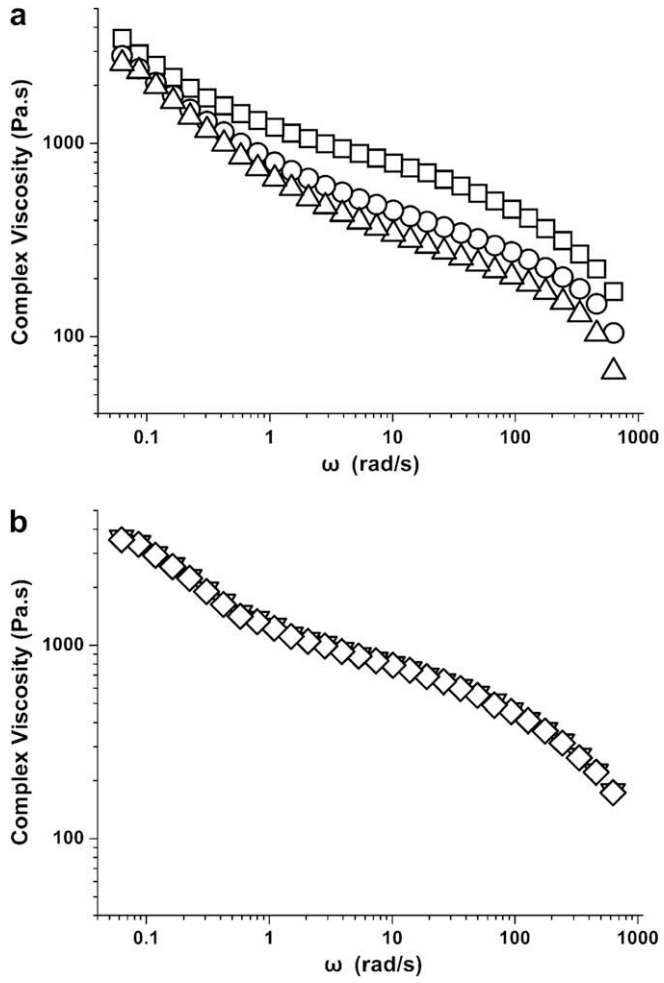

Fig. 12. Plots of complex viscosities of PC–ABS/PHBDET as a function of processing duration at 260 °C (a): (□) for 4 min, (△) for 7 min, and (○) for 10 min; and at 240 °C (b): (▽) for 7 min, (◇) for 10 min.

composite showed optimal tensile properties. It could be concluded that 85/15 PC–ABS/PHBDET composite obtained at 260 °C for 7 min melt processing could achieve a good balance of both compatibility and tensile properties.

Table 7
Tensile properties of PC–ABS and squeezed-out flakes of 85/15 PC–ABS/PHBDET composites prepared at 260 °C for 4, 7 and 10 min.

	PC–ABS	4 min	7 min	10 min
Tensile strength (MPa)	44.14 ± 2.75	47.57 ± 2.95	52.79 ± 2.31	42.29 ± 3.17
Tensile modulus (GPa)	2.15 ± 0.16	2.83 ± 0.27	2.80 ± 0.20	2.70 ± 0.24
Elongation at break (%)	30 ± 4	6 ± 2	6 ± 2	7 ± 3

5. Conclusions

In this article we have summarized our results of the investigation on transesterification and relevant mechanical properties of the composites consisting of PC–ABS and PHBDET. ^{13}C NMR was used to examine the extent of transesterification as a function of the melt processing temperature and duration. Results revealed that the extent of transesterification was quite low when the processing temperature is lower than 250 °C, but was improved with increasing the processing temperature and duration. Simultaneously, the transesterification-controlled compatibility of the composite also increased as indicated through DSC and TMDSC results. Morphology observation of the composite indicated that the transesterification played a negative role on the microfibrillation of PHBDET as the compatibility between continuous and separated phases affected much on the interfacial friction of two phases. However, because of the transesterification-controlled compatibility, a certain extent of transesterification showed a positive influence on the tensile properties of the composite. There existed an optimal extent of transesterification which gave rise to both microfibrillation morphology and tensile properties. A composite obtained at 260 °C for 7 min achieved a good balance of both compatibility and tensile properties.

Acknowledgements

This work was financially supported by the National Science Foundation of China (Grant No.20674053) and the National Science Fund for distinguished Young Scholars (50525309). The authors would like to thank the Analysis and Testing Center of Sichuan University for the NMR measurements.

References

[1] Pham HT, Munjal S, Bosnyak CP. Polycarbonate. In: Olabisi O, editor. Handbook of thermoplastics. New York: Marcel Dekker; 1997.
[2] Pham HT, Weckle CL, Ceraso JM. Adv Mater 2000;12:1881–5.
[3] Grabowski TS. US Patent 3130177; 1964.
[4] Paul DR, Barlow JW. J Macromol Sci Rev Macromol Chem 1980;18:109–68.
[5] Suarez H, Barlow JW, Paul DR. J Appl Polym Sci 1984;29:3253–9.
[6] Wildes G, Keskkula H, Paul DR. Polymer 1999;40:7089–107.
[7] George J, Sreekala MS, Thomas S. Polym Eng Sci 2001;41:1471–85 and references quoted therein.
[8] Coleman JN, Khan U, Blau WJ, Gun'ko YK. Carbon 2006;44:1624–52 and references quoted therein.
[9] Coleman JN, Khan U, Blau WJ, Gun'ko YK. Adv Mater 2006;18:689–706. references quoted therein.
[10] Han H, Bhowmik PK. Prog Polym Sci 1997;22:1431–502 and references quoted therein.
[11] Meng FB, Cui Y, Chen HB, Zhang BY, Jia C. Polymer 2009;50:1187–96.
[12] See details: http://www.ticona.com/index/products/liquid_crystal.htm
[13] Kiss G. Polym Eng Sci 1987;27:410–23.
[14] Tiong SC. Mater Sci Eng R 2003;41:1–60 and references quoted therein.
[15] De Gennes PG, Prost J. The physics of liquid crystals. 2nd ed. Oxford: Clarendon Press; 1993.
[16] Tang P, Reimer JA, Denn MM. Macromolecules 1993;26:4269–74.
[17] Bafna SS, Sun T, De Souza JP, Baird DG. Polymer 1995;36:259–66.
[18] Wei KH, Jang HC, Ho JC. Polymer 1997;38:3521–32.
[19] Flory PJ. Principles of polymer chemistry. Ithaca: Cornell University Press; 1953.
[20] Kotilar AM. J Polym Sci Macromol Rev 1981;16:367–95.
[21] Wu C, Han CD, Suzuki Y, Mizuno M. Macromolecules 2006;39:3865–77.
[22] Guo M, Zachmann HG. Polymer 1993;34:2503–7.
[23] Guo M, Brittain WJ. Macromolecules 1998;31:7166–71.
[24] Su KF, Wei KH. J Appl Polym Sci 1995;56:79–89.
[25] Wei KH, Su KF. J Appl Polym Sci 1996;59:787–96.
[26] Wei KH, Ho JC. J Appl Polym Sci 1997;63:1527–33.
[27] Wei KH, Ho JC. Macromolecules 1997;30:1587–93.
[28] Ho JC, Wei KH. Polymer 1999;40:717–27.
[29] Tovar G, Carreau PJ, Schreiber HP. Colloids Surf A 2000;161:213–23.
[30] Wu L, Chen P, Zhang J, He J. Polymer 2006;47:448–56.
[31] Tan LP, Yue CY, Tam KC, Lam YC, Hu X, Nakayama K. J Polym Sci Part B Polym Phys 2003;41:2307–12.
[32] Jin JI, Antoun S, Ober C, Lenz RW. Br Polym J 1980;12:132–46.

[33] Antoun S, Lenz RW, Jin JI. J Polym Sci Polym Chem 1981;19:1901–20.
[34] Chen L, Huang HZ, Wang YZ, Jow J, Su K. Acta Polym Sin 2009;5:99–104.
[35] Yu T, Guo M. Prog Polym Sci 1990;15:825–908.
[36] Yamadera R, Murano MJ. J Polym Sci Part A Polym Chem 1967;5:2259–68.
[37] Devaux J, Godard P, Mercier JP. J Polym Sci Part A Polym Chem 1982;20:1875–80.
[38] Zhao CS, Chen L, Wang YZ. J Polym Sci Part A Polym Chem 2008;46:5752–9.
[39] Fox TG. Bull Am Phys Soc 1956;2:123.
[40] Wood LA. J Polym Sci 1958;28:319–30.
[41] Gordon M, Taylor JS. J Appl Chem 1952;2:493.
[42] Yang H, Yetter W. Polymer 1994;35:2417–21.
[43] Song M, Hammiche A, Pollock HM, Hourston DJ, Reading M. Polymer 1995;36:3313–6.
[44] Song M, Hourston DJ, Pollock HM, Hammiche A. Polymer 1999;40:4763–7.
[45] Ding Y, Zhang J, Chen P, Zhang B, Yi Z, He J. Polymer 2004;45:8051–8.
[46] Boles D, Cakmak M, Yalcin B. Polymer 2009;50:3541–53.
[47] Martinez-Gomez A, Perez E, Alvarez C. Polymer 2009;50:1447–55.